Inspection of Copper Heat Exchanger Tubes Using HTS-SQUID

Yoshimi HATSUKADE , Akifumi KOSUGI† and Saburo TANAKA‡

Department of Ecological Engineering, Toyohashi University of Technology, 1-1 Hibarigaoka, Tenpaku-cho, Toyohashi, Aichi, 441-8580 Japan

E-mail: hatukade@eco.tut.ac.jp, †ez013811@mail.eco.tut.ac.jp, ‡tanakas@eco.tut.ac.jp

Abstract Experiments of nondestructive inspection (NDI) on copper heat exchanger tubes using an HTS-SQUID have been conducted. An eddy-current-based NDI system using HTS-SQUID gradiometer cooled using a cryocooler was developed for the detection of micro flaws on thin copper tubes 6.35 mm in diameter and 0.825 mm in thickness. With an excitation field of 1.6 μT at 5 kHz, a 30-um-depth flaw was successfully detected by the system, where the conventional NDI techniques would fail to detect. Numerical simulations were also investigated to know how many sensors would be required for inspection around a whole circumference of a copper tube.

Keyword nondestructive inspection (NDI), HTS-SQUID gradiometer, copper heat exchanger tube, micro flaw, eddy current, cryocooler

1. Introduction

Eddy current testing (ECT) has been employed for detection of flaws occurred on heat exchanger tubes as a nondestructive inspection (NDI) technique for quality control [1-3]. However, as the heat exchanger tubes have been formed thinner than 1 mm for better performance, a new NDI technique with higher sensitivity than conventional ECT systems is required for inspection of very shallow flaws a few tens μm in depth.

Taking advantage of the uncontested high sensitivity, SQUIDs have been applied to NDI on metals and electrically conductive composites for detection of small defects [4-6]. In this study, we constructed an eddy-current-based NDI system applying an HTS-SQUID gradiometer cooled using a cryocooler for copper heat exchanger tubes. The inspection of micro flaws on the tubes was demonstrated using the SQUID-NDI system. Numerical simulations were also studied to know how many sensors would be required for inspection around a whole circumference of a copper tube.

2. NDI method

The NDI method for detection of micro flaws on the copper heat exchanger tubes that we employ is based on eddy current technique. A Helmholtz-like coil composed of two identical field coils is used as an inducer [7]. Figure 1 shows the schematic image of the principle of the detection method. A copper heat exchanger tube under test is moved through a Helmholtz-like coil, which induces an eddy current in the tube while applying an excitation field. In the case of the tube with a flaw, the eddy current is disturbed due to the flaw, and then the disturbed eddy current generates anomalous magnetic signal. An HTS-SQUID gradiometer, which is set at the middle of the Helmholtz-like coil and above the tube, measures the anomalous field gradient generated by the eddy current.

3. SQUID-NDI system

A SQUID-NDI system for inspection of copper heat exchanger tubes was constructed in an electromagnetically shielded room. The system is composed of an HTS-SQUID gradiometer with SQUID electronics, a cryostat with coaxial pulse tube cryocooler (PTC) and motor valve and compressor, Helmholtz-like coil with position adjuster, a current supplier, a lock-in amplifier, an electric slider with a slider controller and a PC. Figure 2 shows the schematic illustration of the system. An HTS-SQUID gradiometer was introduced in order to operate the system in a nearly ambient field. The gradiometer also suppresses the increase in magnetic noise due to the mechanical vibration by the cryocooler. The HTS-SQUID gradiometer is a direct-coupled type, and has differential rectangular pick-up coils. The size of each pick-up coil and the baseline length of the gradiometer are 2.88 mm x 3.6 mm and 3.6 mm, respectively. We employed a compact coaxial PTC with low mechanical vibration amplitude less than 1.5 μm at the cold head to cool the SQUID. The working temperature of the SQUID is around 74 K. The details of the gradiometer and PTC are described elsewhere [8,9]. The magnetic flux noise of the SQUID-NDI system measured in a flux-locked loop (FLL) operation in the eddy-current shielded room is about 70 $\mu\phi_0/Hz^{1/2}$ from 10 Hz to 5 kHz, where $\phi_0 = 2.07 \times 10^{-15}$ Wb is the magnetic flux quantum. Corresponding field

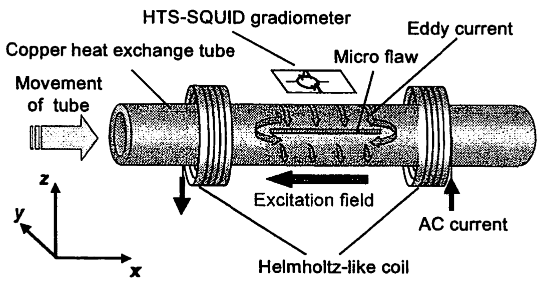

Fig. 1. Principle of the eddy-current based SQUID-NDI method to detect a shallow flaw on a copper tube.

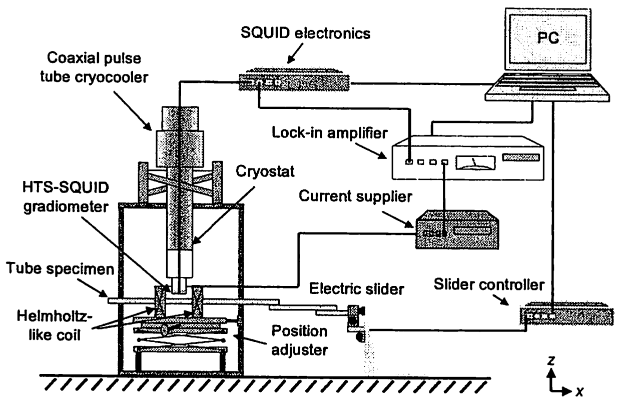

Fig. 2. Schematic diagram of the SQUID-NDI system cooled using a cryocooler for inspection of tube specimen.

gradient noise is about 7 pT/cm/Hz$^{1/2}$. The turn number and dimensions of each field coil of the Helmholtz-like coil are 3000 and 50 mm in diameter and 42 mm in length, respectively. The field coils are separated with a distance of 44 mm between each coil end while aligning the center of each coil. The details of the system is described elsewhere [10].

4. Specimens

Three copper heat exchanger tubes that had artificial micro flaws on surfaces were prepared as specimens. These tubes were selected from commercial products. The dimensions of all the tubes are 6.35 mm in outer diameter, 0.825 mm in thickness and 300 mm in length. The common dimensions of the flaws are 100 μm in width and 15 mm in length. The depths of the flaws are 100 μm, 50 μm, and 30 μm, respectively. The flaws were made using an electric discharge machine.

5. Inspections

The inspection of the copper heat exchanger tube specimens was demonstrated using the SQUID-NDI system. A sinusoidal current of 5 kHz was applied to the Helmholtz-like coil to generate an excitation field. The magnetic flux density B_x was 1.6 μT at the middle of two field coils. The tube specimens were moved stepwise through the Helmholtz-like coil with a step of 0.3mm. The flaws were set to be closest to the SQUID gradiometer with a lift-off distance 1.5 mm. The amplitude and phase of the field gradient in the x-direction of the vertical magnetic field dB_z/dx were measured using the HTS-SQUID gradiometer (See Fig.1). Before the measurements, the position of the inducer was carefully adjusted relative to the gradiometer to minimize the SQUID output due to the excitation field itself. The experimental results on the tube specimens with 100-μm-, 50-μm-, and 30-μm-depth flaws using the excitation field at 5 kHz are shown in Fig. 3. For the reference, the same-dimensional *flawless* copper tube was also measured, and the result is plotted in Fig. 3 (a). In each figure, a cross-sectional view of the tube specimen is depicted together. Except the result on the flawless specimen, anomalous signals due to the micro flaws appear above the

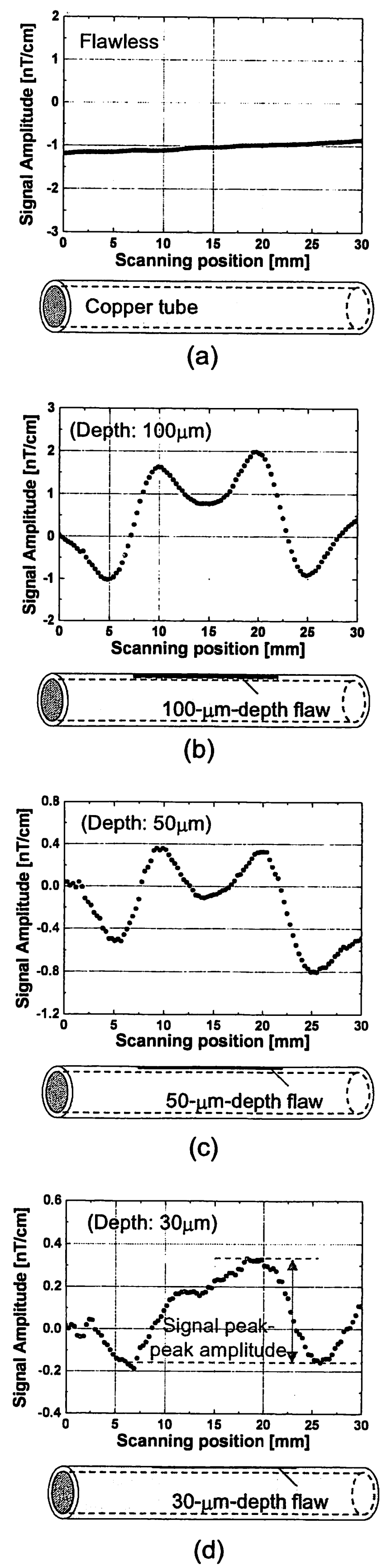

Fig. 3. Measurement results. (a) Flawless, (b) 100-μm-depth flaw, (c) 50-μm-depth flaw, and (d) 30-μm-depth flaw.

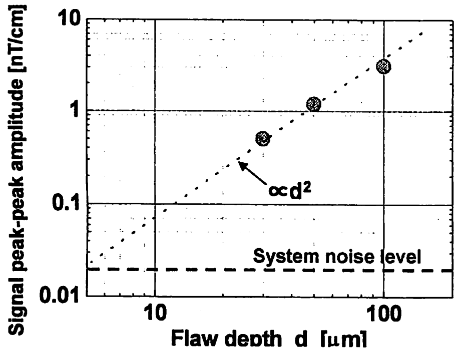

Fig. 4. Relationship between a flaw depth and a signal peak-peak amplitude due to the flaw.

flaws. As shown in Fig. 3 (d), the 30-µm-depth flaw, which conventional methods should fail to detect, was successfully detected with an SN ratio of at least 20. Figure 4 shows the relationship between the flaw depth and peak-peak amplitude of the field gradient signal due to the flaw. We defined the peak-peak amplitude as shown in Fig. 3 (d). The signal amplitude decreases by a factor of d^2 as the flaw depth decreases, where d is the flaw depth [10]. With consideration of this relationship and the sensitivity of the system, the experimental results indicate that the SQUID-NDI system has a potential to detect sub-10-µm-depth flaws.

6. Simulations

As for the above-mentioned experiments, all flaws were located to be closest to the SQUID. However, as for the real situations, flaws do not always locate at the top of the tube. Thus, we investigated how the magnetic signal due to a flaw would change in the case that the flaw did not locate closest to the SQUID by numerical simulation. Figure 5 shows the simulation model that we employed. The left drawing in the figure shows the cross-sectional image of a tube with a flaw. In this simulation, we assumed that the magnetic field generated by an eddy current disturbed due to a flaw could be approximated with a magnetic field generated by virtual current dipoles on the position of the flaw. As shown in the figure, a current dipole has a current moment **Q**. We defined the angle θ is the angle from the xz-plane to the flaw in the yz-plane. The magnetic field **B**(**r**) at the measurement point **r** was calculated using the following equation,

$$\mathbf{B}(\mathbf{r}) = \frac{\mu_0}{4\pi}\sum_i \frac{\mathbf{Q}\times(\mathbf{r}-\mathbf{r}_i)}{|\mathbf{r}-\mathbf{r}_i|^3} \qquad (1)$$

where μ_0 is the permeability of the air, and $\mathbf{r}_i$ is the vector toward a current dipole while i is the index of a current dipole. The right drawing in Fig. 5 shows the top view of the tube specimen. We assumed that the alignment of the virtual current dipoles on the flaw location was composed of 16 discrete dipoles with separation of 1 mm for simplicity. The current moment Q were assumed to have a amplitude of 240nAm. The dimensions of the flaw were assumed to be 15mm in length, 0.1mm in width, and 0.5mm in depth. The dimensions of a tube specimen were same as the tube used in the experiments. The height of the measurement points was 5mm. Then we calculated the gradient of magnetic field dB_z/dx generated by the alignment of current dipoles at the measurement points as shown in Fig. 5, while rotating the tube toward θ direction stepwise with a step of 15 degree.

Figure 6 shows the simulation results, which give the amplitudes of field gradient as a function of the measurement point on the x-axis with rotation of the tube. Nearly same shape plots as shown in Fig. 3 were obtained. The signal peak-peak amplitude decreases with the increase in rotation angle θ. The signal disappears at θ = 90 degree, because the virtual current dipole completely oriented toward the z-direction and such dipoles generate no magnetic component toward z-direction. When the rotation angle excess 90 degree, the signal appeared again. However, in such cases, the amplitude of the signal became significantly small because the distance $|\mathbf{r}-\mathbf{r}_i|$ increases and the signal decreases by a factor of $|\mathbf{r}-\mathbf{r}_i|^3$ as shown in the Eq. 1.

Figure 7 shows the plot of the signal peak-peak amplitude due to the dipoles versus the rotation angle of the tube. The signal peak-peak amplitudes are normalized by the amplitude at θ=0 degree. If the threshold is determined to be 20 % of the peak-peak amplitude at θ=0 degree as shown in the figure, the plot indicates one sensor can cover the

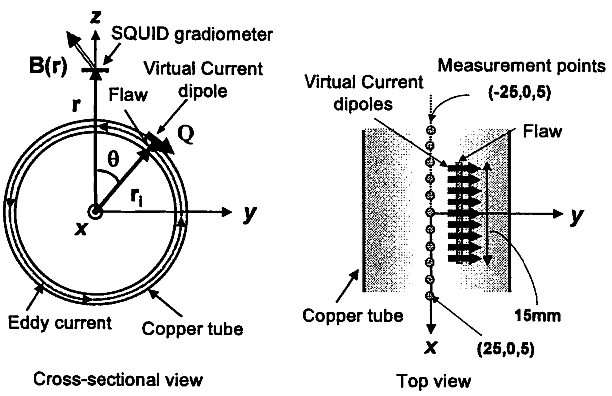

Fig. 5. The simulation model of a copper tube with a flaw in the case that an eddy current is induced in the tube.

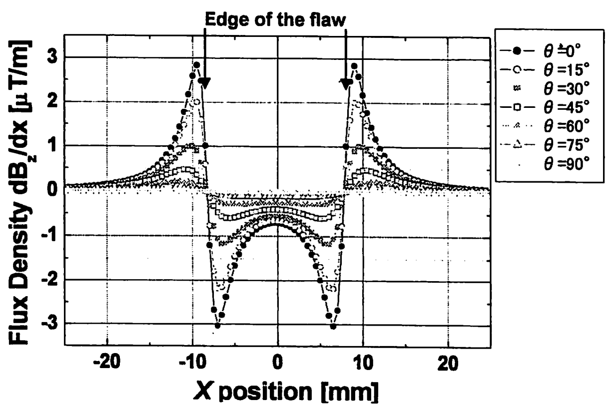

Fig. 6. The simulation results while rotating the tube stepwise with a step of 15 degree from 0 to 90 degree.

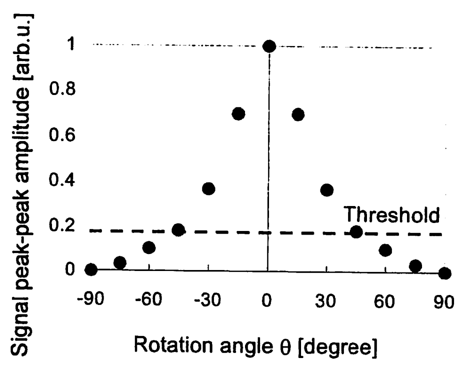

Fig. 7. Signal peak-peak amplitude due to the current dipoles versus the rotation angle of the tube.

rotation angle of the tube about 90 degree. It lead to that 4 or more sensors are necessary for inspection around a whole circumference of a tube in the case that the tube cannot be rotated.

7. Conclusions

The detection of artificial flaws several tens of μm in depth on copper heat exchanger tubes was demonstrated using the eddy-current-based SQUID-NDI system, in which the HTS-SQUID gradiometer was cooled using the cryocooler. With an excitation field of 1.6 μT at 5 kHz, a 30-μm-depth flaw was successfully detected with an SN ratio of about 20. The signal peak-peak amplitude of the signal due to the flaw is approximately proportional to the square of flaw depth. With consideration of the system sensitivity, the results indicate that sub-10-μm-depth flaws are detectable using the SQUID-NDI system.

In addition, the simulation was done to know how the magnetic signal due to a flaw would change in the case that the flaw did not locate closest to the SQUID. The simulation results suggest that several sensors should be required for inspection around a whole circumference of a tube in the case that the tube cannot be rotated.

References

[1] A. J. Trivedi and R. R. Parikh, "In situ eddy current inspection of heat exchanger tubes", Proc. 14th World Conf. Non-Destructive Testing, vol.3, pp.1729-1735, Dec.1996.

[2] K. A. Gopal, N. Raghu, N. G. Muralidharan, P. V. Kumar and K. V. Kasiviswanathan, "Development of calibration standard for non-destructive testing of small diameter tubes", Proc. 14th World Conf. Non-Destructive Testing, Vol.2, pp.663-666, Dec.1996.

[3] H. H. Roasmussen, H. Kristensen, and L. Jeppesen, "NDT and Heat Exchanger Tubes", 7th European Conference On Non-Destructive Testing, Vol.3, pp.739-745, Oct.1996.

[4] H. -J. Krause and M. v. Kreutzbruck, "Recent developments in SQUID NDE", Physica C, Vo.368, pp.70-79, 2002.

[5] Y. Hatsukade, N. Kasai and A. Ishiyama, "Non-destructive detection of delamination in carbon-fiber-reinforced plastics using high-Tc super-conducting quantum interference device", Jpn. J. Appl. Phys., Vol.L606, pp.40-42, 2001.

[6] Y. Hatsukade, M. S. Aly-Hassan, N. Kasai, H. Takashima, H. Hatta, A. Ishiyama, "SQUID-NDE Method on Damaged Area and Damage Amount of Defects in Composite Materials", IEEE Trans. Appl. Supercond., Vol.13, pp.207-210, 2003.

[7] S. Tanaka, T. Mizoguchi, H. Ota and Y. Kondo, "Lymph-node detection system using a high Tc SQUID and ultra-small particles", IEICE Trans. Electron, Vol.E85-C, No.3 pp.687-690, 2002.

[8] Y. Hatsukade, T. Inaba, N. Kasai, Y. Maruno, A. Ishiyama, S. Tanaka, "Detection of Deep-lying Defects in Carbon Fiber Composites Using SQUID-NDE System Cooled by a Cryocooler", Physica C, Vol.412-414P2, pp.1484-1490, 2004.

[9] Y. Hatsukade, N. Kasai, H. Takashima, A. Sakamaki, Y. Maruno, S. Tanaka and A. Ishiyama, "Low-noise Cryocooler-cooled Compact SQUID-NDE System for Carbon-Fiber Composites", to be published in the Proceedings of EUCAS 2003, 2004.

[10] Y. Hatsukade, A. Kosugi, K. Mori and S. Tanaka, "Eddy Current Based SQUID-NDI System for Thin Copper Tubes", Jpn. J. Appl. Phys., Vol.43, No.11B, pp. L1488-L1491, Nov.2004.